Realization of a causal-modeled delayed-choice experiment using single photons

Shang Yu,[1,2] Yong-Nan Sun,[1,2] Wei Liu,[1,2] Zhao-Di Liu,[1,2] Zhi-Jin Ke,[1,2] Yi-Tao Wang,[1,2,*] Jian-Shun Tang,[1,2,†] Chuan-Feng Li,[1,2,‡] and Guang-Can Guo[1,2]

[1] *CAS Key Laboratory of Quantum Information, University of Science and Technology of China, Hefei, 230026, China*
[2] *Synergetic Innovation Center of Quantum Information and Quantum Physics, University of Science and Technology of China, Hefei, 230026, P.R. China*

(Dated: March 5, 2022)

Wave-particle duality constitutes one of the most intriguing features in quantum physics. A well-known gedanken experiment that provides evidence for this is the Wheeler's delayed-choice experiment based on a Mach-Zehnder interferometer. Many different versions of delayed-choice experiments have been conducted with both classical and quantum detecting devices. Recently, it was proposed that the delayed-choice experiment could be devised from the perspective of device-independent prepare-and-measure scenario. In our work, we experimentally realize this modified version with a deterministic single-photon source, and examine the wave-particle objective in a causal-modeled scheme without assistance of entanglement, which is achieved by violating the dimension witness inequalities. Our experiment also provides an intriguing perspective and exhibits the benefits of studying quantum theory from the casual model point of view.

Introduction.—The wave-particle duality is a central concept in quantum mechanics. The young's double-slit interference experiment [1] is a celebrated example in which the concept of duality plays an important role in the famed Bohr-Einstein debate and prompted Bohr to formulate the complementarity principle [2]. Bohr's complementarity principle states that a single quantum object can behave as a wave or as a particle depending on the measurement apparatus. However, an alternative view of complementarity assumes that the particle somehow knows the type of detecting device and adjust its own behavior before entering the apparatus. To examine this idea, Wheeler proposed the delayed-choice gedanken experiment where the choice of the property that will be observed is made after the photon has passed the first beamsplitter of a Mach-Zehnder interferometer: "Thus one decides the photon shall have come by one route or by both routes after it has already done its travel" [3–5].

Since Wheeler's delayed-choice experiment (WDCE) was proposed, many modified versions of this experiment have been conducted [6–9]. The original version of this experiment was first realized using a fast electronic device[10, 11]. Subsequently, a quantum version of the delayed-choice experiment (QDCE) was proposed by Ionicioiu and Terno (IT) [12] in a particular wave-particle objective model, where they replaced the second beamsplitter in WDCE with a quantum controlled one that could exist in a superposition of being present or absent until after the photon is detected. Ascertaining whether the beam splitter was truly in a quantum superposition state motivated entanglement-assisted QDCE [13–15] which relied on the violation of a Bell inequality to rule out the IT model in a device-independent (DI) manner [16, 17]. Moreover, Tang *et al.* [18] observed the quantum wave-particle superposition through the interference fringes directly and proved that the quantum wave-particle superposition state was distinct from the classical mixture state because of the quantum interference between the wave and particle states.

Recently, a new proposal [19] based on the causal model demonstrated that a two-dimensional classical hidden variable model could explain the outcomes of WDCE and QDCE. Herein, the delayed-choice experiments could be considered from the perspective of device-independent causal models in a prepare-and-measure scenario. Furthermore, this proposal could exclude any two-dimensional nonretrocausal classical model in a device-independent manner based on the violation of the dimension witness inequality [20, 21].

In this Letter, we experimentally realize this causal-modeled delayed-choice experiment with a deterministic single-photon source. In order to test the wave-particle objectivity, we examine whether the hidden variable model has the same dimension as the quantum system we test. Based on the widely-used dimension witness inequalities, we can exclude any two-dimensional nonretrocausal classical hidden variable model in a DI manner through our experimental results and without help of entanglement. We first test the dimension witness $|\mathrm{Det}(W_2)|$ for uncorrelated preparation and measurement devices where the preparation and the measurement are affected by two independent noise terms [19, 20]. This method is highly robust to technical imperfections and can be used in the presence of arbitrary noise and low detection efficiency, which indicates we can test this causal-structured delayed-choice experiment in a detection loophole-free manner. Secondly, the dimension witness I_{DW} can be obtained when the preparation and the measurement are allowed to be correlated via shared randomness. Our experimental results also show we can violate the dimension witness inequality in this case. Finally, we measure the retrocausality quantities at different preparation settings, and show how much retrocausality that would be required to reproduce the quan-

tum experimental results. The experimental data used to violate the dimension witness inequalities can also deduce to the Hanbury-Brown and Twiss (HBT) [22] outcome at the same time by different data processing method, which proves the single-photon property of our source. Our work demonstrates a WDCE in the DI "prepare-and-measure" scenario, and shows an advantage of studying quantum theory from the causal perspective.

Brief review of the causal model.—As shown in Fig. 1(a), the causal relationships between n random variables $(X_1, ..., X_n)$ can be graphically described by directed acyclic graphs (DAGs), where each node in the graph represents a variable and each directed edge represents a causal relation between two variables. The causal model in Fig. 1(a) implies that any observed distribution compatible with a hidden variable (HV) causal model should be factorized as $p(d|x,y) = \sum_\lambda p(d|y,\lambda)p(\lambda|x)$. Under the assumption of non-retrocausality, the variables Y and Λ should be statistically independent. When retrocausality is allowed, there will be causal influence between the variables Y and Λ. In Ref. [19], Chaves *et al.* proposed that the delayed-choice experiment can be regarded as a DI prepare-and-measure (PAM) scenario (Fig. 1(b)). When pressing button X, the state preparator emits a particle in the state $\rho(x)$. Then the emitted particles are sent to the measurement device in order to perform the action of witness. When button Y is pressed, the measurement device performs the measurements on the incoming particles and produces the outcomes. The quantum experimental results is thus described by the probability distribution $p(d|x,y)$ which can be written in the form $p(d|x,y) = \mathrm{Tr}(\rho(x)M_{d|y})$ for the state $\rho(x)$ and measurement operator $M_{d|y}$ ($\Sigma_d M_{d|y} = \mathbb{I}$).

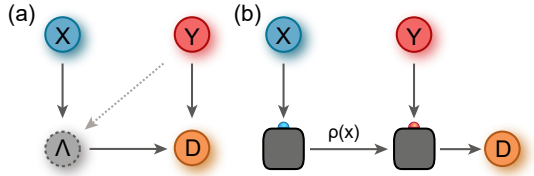

FIG. 1: Causal model and PAM scenario for the delayed-choice experiment. (a) DAG representation of the causal structures for the delayed-choice experiment. Under the assumption of non-retrocausality (neglecting the grey dash line), the variables Y and Λ should be statistically independent. When the retrocausality is allowed (including the grey dash line), there will be causal influence between the variables Y and Λ. (b) Device-independent scenario for testing the delayed-choice experiment. When button X is pressed, the state preparator emits a particle in a state $\rho(x)$, and it will be sent to a measurement device. When button Y is pressed, the device performs measurement on the particle and the measurement produces outcomes D.

Experimental setup and results.—The experimental setup for the causal-modeled delayed-choice experiment is illustrated in Fig. 2. Single photons generated from an hBN sample (see Supplemental Materials [25] for details) serve as the photon source for the experiment, which lies at the top platform in this figure. First, the photons will pass through a beam splitter (BS1), which is constituted by a polarizing beam splitter (PBS), a half wave plate (HWP) at 22.5° and a beam displacer (BD), and then enter into a Mach-Zehnder (MZ) interferometer. After the photons enter into the interferometer, a fixed phase φ_{x_i} is immediately applied on the path a at the preparation stage, which is realized by tilting the corresponding glass plate. Then, the photons are delayed by 300 ns through a 60 m long optical fiber, which also delivers the path state $\rho(x) = |\psi(x)\rangle\langle\psi(x)|$, $|\psi(x)\rangle = 1/\sqrt{2}(|b\rangle + e^{i\varphi_{x_i}}|a\rangle)$ to the measurement stage. It is to be noted that before a photon enters into the fiber, difference of the optical length of two paths is far greater than coherent time of the photon. Thus the fiber can be split into two isolated channels corresponding to paths a and b, according to both the coherent-time separation and polarization separation. Namely, paths a and b in the MZ still maintain, but only propagate in a same spatial position. An attenuator in path a is used to adjust the transmittance T_a artificially. The measurement bases, Y_1 or Y_2, are chosen independently by a quantum random switch (QRS), and its concrete setup is shown in the dashed line frame at the bottom of Fig. 2. The randomness of QRS is ensured by a quantum random number generator (QRNG) [23]. The input photon in QRS is already at the horizontal polarization for both paths since we already rotated the vertical component by a HWP at 45°. The photon then goes through a HWP at 22.5°, and is focused by a convex lens pair (focal length f = 300 mm) into the spatial electro-optic modulator (EOM). EOM provides a phase shift of 0 or π between the horizontal and vertical polarization according to the signal generated by QRNG. Another HWP at 22.5° rotates the polarization again, and a PBS after that can choose (according to the QRNG output) the photon to go which measurement stage independently of the preparation. The QRS can ensure that the choice of measurement base Y does not have any causal influence from the preparation X [24], and assist in obtaining a fast phase shift on the path degree of freedom. More details about QRS are presented in the Supplemental Materials [25]. The phase shift σ_{y_1} or σ_{y_2} applied on path b at the measurement stage is realized by tilting the glass plate, which is similar to the preparation. The phase plates (PP) in BS2 are used to compensate for undesirable phase disturbances induced by optical elements. A single photon avalanche diode after BS2 detects the photons, which are then analyzed by a time-to-digital converter (TDC, ID Quantique, ID800) to obtain both the dimension witness results and the second-order time correlation of the single photon source (SPS) simultaneously.

Fig. 3 shows the antibunching result of the SPS we obtain in the experiment. Results reveal that $g^{(2)}(0) =$

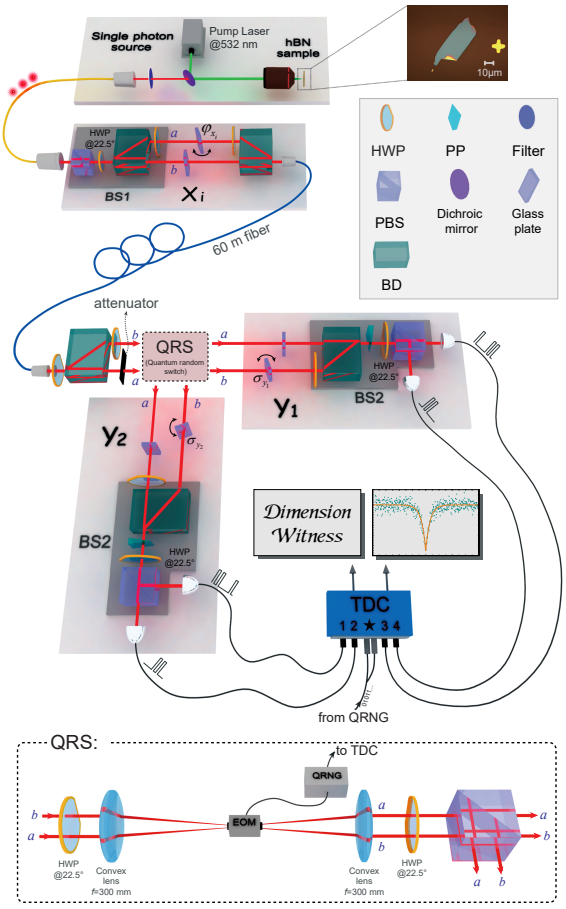

FIG. 2: Experimental setup. The single photon source is generated from hBN sample that is pumped by a 50 μW 532 nm laser. After the photon enters into the interferometer (at BS1), a fixed phase φ_{x_i} is applied on path a by tilting corresponding glass plate at the preparation stage. The photon is then delayed 300 ns by a 60 m long fiber (the optical length before the fiber is unbalanced, and the fiber can be split into the two isolated channels from both the polarization and coherence-time perspective). The attenuator in path a is applied for adjusting the transmittance. A QRNG-based switch (QRS) inside the interferometer enables the measurement bases to be chosen independently. Two phases on the measurement stage σ_{y_1}, σ_{y_2} are realized by glass plates similar to the φ_{x_i} at preparation stage, and the photon then is detected after BS2. The HWPs are all rotated at 45° if there are no special notes. Then the dimension witness results can be calculated from the coincidence events from the ports 1,2,★ for stage Y_1 or from the ports 3,4,★ for stage Y_2, respectively. The second-order-correlation of SPS, can also be obtained by the total counts from the same data record (ports 1-4, without port ★).

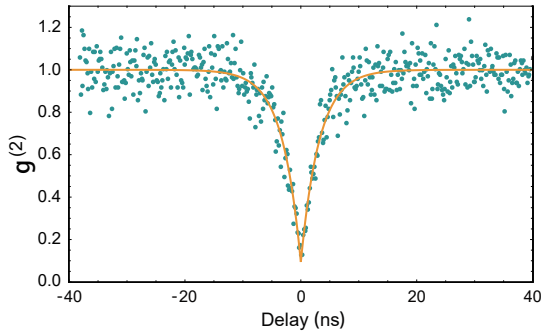

FIG. 3: The antibunching result of the SPS that is derived from the same data in experiment. The green dots are the normalized coincidence-counting results, and the orange line is the theoretical fit for the data. The fitting function for the second-order time correlation is $g^{(2)}(t) = 1 - \alpha e^{-|t|/\tau}$ where t is the time delay, α and τ are the fitting parameters. The fitting results show the lifetime $\tau = 3.193 \pm 0.136$ ns.

0.093 ± 0.025, and the single photon purity then is $\sqrt{1 - g^{(2)}(0)} = 0.952$ [26], which indicates 4.8% probability of multi-photon generation in experiment. This demonstrates a remarkable quantum emission performance and the high single-photon purity at room temperature (more details can be found in Supplemental Materials [25]).

In order to test the wave-particle objectivity in our delayed-choice experiment, we try to rule out the two-dimensional causal-structured classical HV models, with the help of the violation of the dimension witness inequalities. Firstly, under the condition that the preparation and measurement devices are uncorrelated, the dimension witness $|\mathrm{Det}(W_2)|$ is tested in a DI manner. Consider a scenario with $2k$ preparations and k binary measurements, we construct the $k \times k$ matrix [20]

$$\mathbf{W}_k(i,j) = p(2j,i) - p(2j+1,i) \tag{1}$$

with $0 \leqslant i,j \leqslant k-1$, we write $p(x,y) = p(d=0|x,y)$ for simplicity.

Since the dimension of the HV models is two, 4 preparations $\{X_i, i = 1 \sim 4\}$ and 2 measurements $\{Y_i, i = 1 \sim 2\}$ are required to if we try to rule out the nonretrocausal classical hidden variable models. Thus, the matrix of interest (1) is given by

$$W_2 = \begin{pmatrix} p(0,0) - p(1,0) & p(2,0) - p(3,0) \\ p(0,1) - p(1,1) & p(2,1) - p(3,1) \end{pmatrix}. \tag{2}$$

We can find that in two dimensional classical hidden variable model, the dimension witness $|\mathrm{Det}(W_2)| = 0$. In our experiment, the transmittance of path a is manipulated in the interferometer, and the statistics is given by $p(x,y) = \frac{1}{4}(T_a^2 + 1) + (T_a/2)\cos(\varphi_x - \sigma_y)$. The experimental results of the dimension witness are shown in Fig. 4(a). Here, 4 preparation bases $\varphi_{x_i} = \{0, \pi, -\pi/2, \pi/2\}$, and 2 measurement bases $\sigma_{y_i} = \{\pi/2, 0\}$ are chosen. Due to the nature of this dimension witness method, we can obtain the violation under any non-zero transmittance T_a (this is equivalent to a non-ideal detection efficiency situation, i.e., $\eta < 1$). By varying T_a, we find that as long as T_a is greater than zero, dimension witness $|\mathrm{Det}(W_2)| > 0$

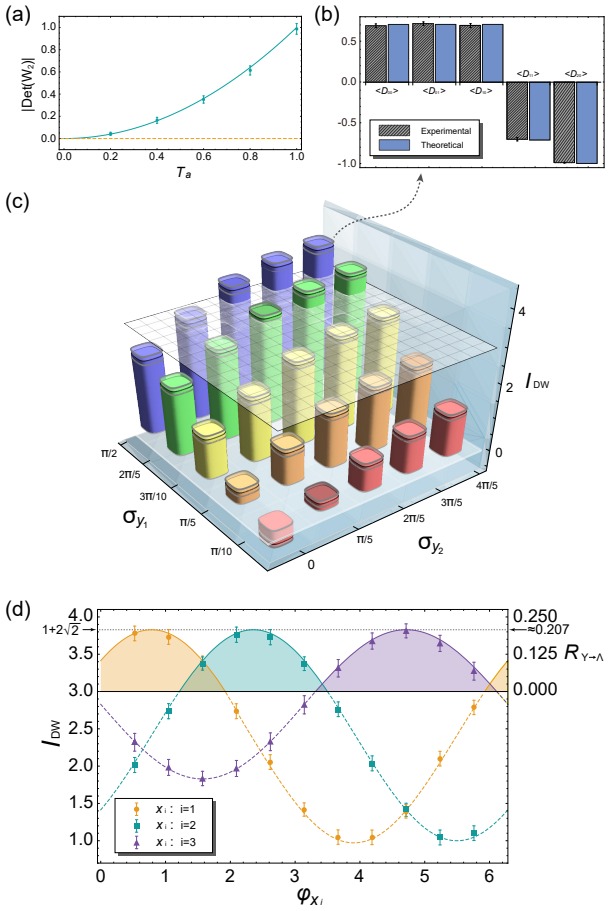

FIG. 4: Experimental results of the dimension witness tests. (a) Experimental results of the dimension witness $|\mathrm{Det}(W_2)|$ when the real transmittance coefficients T_a of one path of the MZ interferometer is varied. (b) Results of the dimension witness I_{DW} at the maximal violation setting. Theoretical and experimental values of $\langle D_{00}\rangle$,$\langle D_{01}\rangle$,$\langle D_{10}\rangle$,$\langle D_{11}\rangle$,$\langle D_{20}\rangle$ are illustrated, which are the terms in the dimension witness I_{DW} with maximal violation. The error bars representing one standard deviation which are obtained from 30 identical experimental procedures. (c) Experimental results of the dimension witness I_{DW} with fixed phase (φ_{x_i}) at preparation stage and different measurement settings. The error range of the data is represented by the two gray edges. (d) The relationship between φ_{x_i} and the retrocausality R. The lines with different colors are the theoretical values when one of the phase shifts (φ_{x_i}) is changed at the preparation. The orange circles, green squares and purple triangles with error bars denote the corresponding experimental values.

always exists. For the condition of $T_a = 1$, the maximal violation $|\mathrm{Det}(W_2)| = 0.987 \pm 0.048$ can be obtained. These results indicate that the PAM scenario can robustly rule out the classical hidden variable model in a DI manner, and not be affected by noise and detection efficiency.

As a complementary, the HV models by another dimension witness I_{DW} are also tested for which the preparation and measurement devices are allowed to be correlated via shared randomness. The employed dimension witness inequality can be written as [21]

$$I_{\mathrm{DW}} = \langle D_{00}\rangle + \langle D_{01}\rangle + \langle D_{10}\rangle - \langle D_{11}\rangle - \langle D_{20}\rangle \leqslant 3. \tag{3}$$

The experimental results of the dimension witness I_{DW} are shown in Fig. 4(b) and Fig. 4(c). In Fig. 4(c), 3 phase shifts φ_{x_i} as $\pi/4, 3\pi/4, -\pi/2$ are fixed at the preparation stage, and the measurement basis $Y1$ and $Y2$ is changed. From a selection of 25 examples from $\sigma_{y1} \in [0, \pi/2]$ and $\sigma_{y2} \in [0, \pi]$, only in some measurement pairs, I_{DW} can be violated. The maximal violation is obtained when we set $\sigma_{y1} = \pi/2$ and $\sigma_{y2} = 0$. In this case, we obtain $I_{\mathrm{DW}} = 3.787 \pm 0.103$, and it is violated by 7.6 standard deviations. The data for each value of $\langle D_{ij}\rangle$ contained in dimension witness I_{DW} is shown in Fig. 4(b).

Besides, the possibility of retrocausality must be allowed if these violation results need to be simulated by binary classical hidden variable model. In Ref. [19], the authors proposed a retrocausality quantifier which has a direct relationship with I_{DW}. This degree of retrocausality R measurement is given by

$$\min\ R_{Y\to\Lambda} = \max[\frac{I-3}{4}, 0]. \tag{4}$$

Thus, according to the maximally violated I_{DW} obtained above, we can find the corresponding $R_{Y\to\Lambda} = 0.197 \pm 0.026$. The experimental results of the retrocausality $R_{Y\to\Lambda}$ under different preparations X_i are shown in Fig. 4(d). In order to determine the relationship between the preparations and the degree of retrocausality, we fix the measurement at the optimal one that is found in Fig. 4(c) (i.e., $\sigma_{y_1} = 0$, $\sigma_{y_2} = \pi/2$), and change the phase shift φ_{x_i} at the preparation stage. For example, when φ_{x_1} is changed, $\varphi_{x_{2,3}} = 3\pi/4, -\pi/2$ is kept fixed. By varying each phase shift in preparation individually, we can find within a complete period, the values of retrocausality $R_{Y\to\Lambda}$ are strongly influenced by preparations, and always below the threshold of 0.207 within the corresponding error.

Conclusion.—In this work, we experimentally realize a causal-modeled delayed-choice experiment using SPS, and perform it with a MZ interferometer under path degree of freedom. For ensuring the delayed-choice requirement in the measurement stage, we build a QRS assisted by QRNG, which can select the measurement bases independent of preparation, and provides a fast phase shift at the measurement stage on the path degree of freedom. In order to test the wave-particle objectivity, in our experiment, based on the two kinds of dimension witness inequalities, $|\mathrm{Det}(W_2)|$ and I_{DW}, we try to exam whether the statistics property of our results is compatible with any binary classical hidden variable model. According to our experimental results, we can exclude any two-dimensional nonretrocausal classical models on account

of the violation of the dimension witness inequalities. Especially, results from the dimension witness inequality $|\mathrm{Det}(W_2)|$ are highly robust to technical imperfections under any non-zero detection efficiency, which can make the test be performed in a DI manner. Meanwhile, the outcomes obtained by I_{DW} can also be applied to quantify the retrocausality, which exhibits how much information from Y to Λ (as shown in Fig. 1) that HV model required to reproduce the quantum experimental results. In addition, results from our experiment also provides an intriguing perspective and reveals that the causal perspective can benefit studies in quantum theory.

This work is supported by the National Key Research and Development Program of China (No. 2017YFA0304100), the National Natural Science Foundation of China (Grants Nos. 11822408, 11674304, 61327901, 61490711, 11774334, 11774335, 11474267, 11821404, 11574291 and 91321313), the Key Research Program of Frontier Sciences of the Chinese Academy of Sciences (Grant No. QYZDY-SSW-SLH003), Anhui Initiative in Quantum Information Technologies (AHY020100, AHY060300), the Youth Innovation Promotion Association of Chinese Academy of Sciences (Grants No. 2017492), the Foundation for Scientific Instrument and Equipment Development of Chinese Academy of Sciences (No. YJKYYQ20170032), the Fundamental Research Funds for the Central Universities (No. WK2470000026), the National Postdoctoral Program for Innovative Talents (Grant No. BX20180293).

S. Yu, Y.-N. Sun and W. Liu are contributed equally to this work.

Note added. When we almost finished the manuscript of our experiment, we noticed similar works by E. Polino *et al*. [27] and H.-L. Huang *et al*. [28], which were carried out simultaneously and independently.

* Electronic address: yitao@ustc.edu.cn
† Electronic address: tjs@ustc.edu.cn
‡ Electronic address: cfli@ustc.edu.cn

[1] R. P. Feynman, R. B. Leighton, M. L. Sands, Lectures on Physics (Addison-Wesley, Reading, MA, 1965).
[2] N. Bohr, in Quantum Theory and Measurement, edited by J. A. Wheeler and W. H. Zurek (Princeton University Press, Princeton, NJ, 1984), pp. 9-49.
[3] J. A. Wheeler, in Mathematical Foundations of Quantum Theory (eds Marlow, A.R.) 9-48 (Academic Press, 1978).
[4] J. A. Wheeler, in Quantum Theory and Measurement (eds Wheeler, J. A., Zurek, W. H.) 182-213 (Princeton University Press, 1984).
[5] A. J. Leggett, in Compendium of Quantum Physics (eds Greenberger, D., Hentschel, K., Weinert, F.) 161-166 (Springer, 2009).
[6] B. J. Lawson-Daku, *et al.*, Delayed choices in atom Stern-Gerlach interferometry, Phys. Rev. A **54**, 5042-5047 (1996).
[7] Y. H. Kim, R. Yu, S. P. Kulik, Y. Shih, and M. O. Scully, Delayed 'choice' quantum eraser, Phys. Rev. Lett. **84**, 1-5 (2000).
[8] T. Hellmut, H. Walther, A. G. Zajonc, W. Schleich, Delayed-choice experiments in quantum interference, Phys. Rev. A **35**, 2532-2541 (1987).
[9] J. Baldzuhn, E. Mohler, W. A. Martienssen, Wave-particle delayed-choice experiment with a single-photon state, Z. Phys. B **77**, 347-352 (1989).
[10] V. Jacques, *et al.*, Experimental realization of Wheeler's delayed-choice gedanken experiment, Science **315**, 966-968 (2007).
[11] V. Jacques, *et al.*, Delayed-choice test of quantum complementarity with interfering single photons, Phys. Rev. Lett. **100**, 220402 (2008).
[12] R. Ionicioiu, and D. R. Terno, Proposal for a quantum delayed-choice, Phys. Rev. Lett. **107**, 230406 (2011).
[13] R. Ionicioiu, T. Jennewein, R. B. Mann, and D. R. Terno, Is wave-particle objectivity compatible with determinism and locality?, Nat. Commun. **5**, 4997 (2014).
[14] R. Rossi, Restrictions for the causal inferences in an interferometric system, Phys. Rev. A **96**, 012106 (2017).
[15] A. S. Rab, E. Polino, Z.-X. Man, N. Ba An, Y.-J. Xia, N. Spagnolo, R. Lo Franco, and F. Sciarrino, Entanglement of photons in their dual wave-particle nature, Nat. Commun. **8**, 915 (2017).
[16] F. Kaiser, T. Coudreau, P. Milman, D. B. Ostrowsky, and S. Tanzilli, Entanglement-enabled delayed-choice experiment, Science **338**, 637 (2012).
[17] A. Peruzzo, P. Shadbolt, N. Brunner, S. Popescu, and J. L. O'Brien, A quantum delayed-choice experiment, Science **338**, 634 (2012).
[18] J.-S. Tang, Y. Li, X. Xu, G. Xiang, C. Li, and G. Guo, Realization of quantum Wheeler's delayed-choice experiment, Nat. Photonics **6**, 602 (2012).
[19] R. Chaves, G. B. Lemos, and J. Pienaar, Causal Modeling the Delayed-Choice Experiment, Phys. Rev. Lett. **120**, 190401 (2018).
[20] J. Bowles, M. T. Quintino, and N. Brunner, Certifying the dimension of classical and quantum systems in a prepare-and-measure scenario with independent devices, Phys. Rev. Lett. **112**, 140407 (2014).
[21] R. Gallego, N. Brunner, C. Hadley, and A. Acín, Device-independent tests of classical and quantum dimensions, Phys. Rev. Lett. **105**, 230501 (2010).
[22] R. Hanbury Brown, and R. Q. Twiss, The question of correlation between photons in coherent light rays, Nature **178**, 1447 (1956).
[23] J.-S. Tang, *et al.*, Experimental investigation of the no-signalling principle in parity¨Ctime symmetric theory using an open quantum system, Nat. Photon. **10**, 642 (2016).
[24] The choice of measurement stage in QRS needs a response time that around 170 ns (i.e., the phase-shift execution in EOM is 170 ns later than the random number generated), which is shorter than the delay time after the phase applied on path a (300 ns).
[25] Supplemental Materials.
[26] R. Brouri, A. Beveratos, J.-P. Poizat, and P. Grangier, Photon antibunching in the fluorescence of individual color centers in diamond, Optics Letter, **25**, 17 (2000).
[27] E. Polino, *et al.*, Device independent certification of a quantum delayed choice experiment, http://arxiv.org/abs/1806.00211 (2018).

[28] H.-L. Huang, *et al.*, A loophole-free Wheeler-delayed-choice experiment, http://arxiv.org/abs/1806.00156 (2018).